Journal of Fluorescence, Vol. 10, No. 1, 2000

Unusual Pathways of Triplet State Dynamic Relaxation in *Meso*-Aryl-Substituted Porphyrins and Their Chemical Dimers at 295 K

V. N. Knyukshto,[1] E. I. Zenkevich,[1,2] E. I. Sagun,[1] A. M. Shulga,[1] and S. M. Bachilo[1]

Received December 11, 1998; accepted November 17, 1999

It was found that mono- and di-*meso*-phenyl substitution in octaethylporphyrins (OEP)and their chemical dimers with the phenyl ring as a spacer manifests itself in the dramatical shortening of T_1 state lifetimes at 295 K (from ~1.5 ms down to 2–5 μs in degassed toluene solutions). On the other hand, this substitution does not influence spectral-kinetic parameters of S_0 and S_1 states. The enhancement of the T_1 state non-radiative deactivation is explained by torsional librations of the phenyl ring around a single C-C bond in sterically encumbered OEP molecules leading to non-planar dynamic distorted conformations in the excited T_1 states. For these compounds with electron-accepting NO_2-groups in the *meso*-phenyl ring the strong non-radiative deactivation of S_1 and T_1 states (by ~2–3 orders of magnitude) is observed upon the displacement of NO_2-group from *para*- to *ortho*-position of the phenyl ring. The S_1 state quenching is caused by the direct intramolecular electron transfer to low-lying CT state of the radical ion pair (the normal region, non-adiabatic case presumably, $V = 130–190\ cm^{-1}$ in dimethylformamide). The additional deactivation of the T_1 state is connected with thermally activated transitions to upper-lying CT states as well as the strengthening of intersystem crossing probabilities.

KEY WORDS: Octaethylporphyrins; *meso*-phenyl; electron-accepting NO_2-groups; S_1 and T_1 state quenching; non-planar conformations; electron transfer.

INTRODUCTION

Synthetic porphyrins and their dimers, covalently linked to various electron acceptors are widely used to model some aspects of photosynthetic electron transfer (ET) events [1]. In some cases, in order to understand ET pathways through bond or through space the porphyrin-acceptor molecule contains an inserted phenyl ring between the redox pair [2–5]. Thus, for the decision whether or not the inserted phenyl ring acts as a stepping stone in ET, it is necessary to test the role of a phenyl ring itself in the deactivation of porphyrin excited S_1 and T_1 states. Recently, the specific role of steric interactions of *meso*-phenyls with flanking β-CH_3 pyrrole substituents was mentioned for ET processes in carotenoid-porphyrin-quinone triads [4]. In this respect it should be noted that the addition of bulky substituents of various nature in *meso*-positions of tetrapyrrole macrocycle leads to the formation of sterically encumbered porphyrins in which deformations from planarity in both S_0 and S_1 states are accompanied by pronounced changes of optical, photophysical and redox properties of tetrapyrrole compounds [6–9]. The conformational dynamics of non-planar tetrapyrrole macrocycle at 295 K manifests itself in large

[1] Institute of Molecular & Atomic Physics, National Academy of Sciences of Belarus, 220072 Minsk, Belarus.

[2] To whom correspondence should be addressed at Laboratory of Molecular Photonics, Institute of Molecular and Atomic Physics, National Academy of Sciences of Belarus, F. Skaryna Avenue 70, 220072 Minsk, Belarus. Fax: +375 172 84 0030. e-mail: zenkev@imaph.bas-net.by

1053-0509/00/0300-0055$18.00/0

bathochromic absorption/fluorescence shifts ($\Delta\nu \approx 1100$ cm^{-1}), the increase of Stokes shift between $Q_x(0,0)$ absorption and fluorescence bands ($\Delta\nu_s \sim 900$ cm^{-1}) and broad emission profiles in both polar and non-polar solvents as well as in a pronounced decrease of fluorescence quantum yields (φ_F) and lifetime (τ_S) shortening. The decrease of the $S_1 \sim\sim > T_1$ intersystem crossing and the drastic T_1 state lifetime (τ_T) shortening for two types of non-planar tetra-*meso*-substituted porphyrins at 295 K in degassed solutions were described in the only paper known to us [10]. However, the detailed analysis of the excited triplet state parameters for such systems has not been carried out yet.

The strengthening of the non-radiative deactivation of S_1 and T_1 states in tetra-*meso*-substituted porphyrins has been associated with the macrocycle non-planarity in the S_0 state and their dynamic distortion in excited states. From this point of view there was no reason to study mono- and di-*meso*-phenyl-substituted porphyrins since the last-mentioned compounds are planar in S_0 state (both in solution and crystal form). Until recently it was assumed that for these objects the energetics and spectral-luminescent properties of excited S_1 and T_1 states have to be closely similar to those known for planar porphyrins.

Nevertheless, we draw principal attention to the fact that mono- and di-*meso*-phenyl substitution in octaethylporphyrins (free bases and corresponding Zn- and Pd-complexes), as well as the formation of the octaethylporphyrin chemical dimer with the phenyl ring as a spacer, leads to major shortening of triplet lifetimes (by ~300–500 times) at room temperature in degassed toluene solutions without any influence on the spectral-kinetic parameters of S_0 and S_1 states. Therefore, we carried out a comprehensive study of the observed effect on a series of porphyrins and their chemical dimers with a variable structure of *meso*-phenyl substituents in various solvents at 295-77 K. Then, taking into account this specific T_1 state quenching we examined spectral and photophysical properties of *meso*-phenyl derivatives of OEP and their chemical dimers, OEP-Ph-OEP, having covalently linked electron-accepting NO_2 groups in *para*-, *meta*- and *ortho*-positions of the phenyl ring. In this paper we present the results obtained for the compounds of interest and analyze the dynamic relaxation of their excited S_1 and T_1 states with and without electron-accepting NO_2 groups.

EXPERIMENTAL

Octaethylporphyrin (**OEP**) was synthesised and purified by the method described in [11]. 5-*Meso*-aryl-substituted derivatives of **OEP**, etioporphyrin II (**EP II**) and tetramethyldiethylporphyrin (**TMDE**) were synthesised and purified using the method described in [12]. The synthesis of 5,15-diaryl-substituted **OEP** type compounds was carried out based on the method presented in [13, 14]. Porphyrin chemical dimers (free bases and Zn-complexes) were synthesised according to known methods [15–17]. The structures of the compounds without NO_2 groups are shown in Fig. 1. The synthesis, purification and identification of the corresponding compounds with one or two NO_2 groups were carried out using the methods cited in [12–14]. The structures of the *meso*-phenyl-substituted compounds containing covalently linked NO_2 groups in *para*-, *meta*- and *ortho*-positions of the phenyl ring are presented in Fig. 2. Toluene, acetonitrile, acetone, dimethylfomamide (Spectroscopic Grade), glycerol and polymeric acrylic film were used at 295 K, methylcyclohexane and methylcyclohexane-toluene mixture 6:1 were used at 77 K for the preparation of glassy rigid matrixes. Deuterated ethanol C_2D_5OD was used in experiments on porphyrin deuteration.

In order to diminish the influence of annihilation effects on the T_1 state decays in liquid solutions at 295 K, porphyrin concentrations of $\sim 10^{-6}$ M were used. Because of significant quenching of the excited S_1 and T_1 states by dissolved molecular oxygen, the main part of the measurements was carried out for degassed samples (purging down to 10^{-5} torr pressure). All photophysical measurements were completed within a few hours after solution preparation. The main spectral-luminescent data and kinetic parameters for the deactivation of the excited S_1 and T_1 states, as well as quantum yields for singlet oxygen generation, were obtained using commercial and hand-made laboratory equipment described in detail in our previous papers [18–20] where standard samples, necessary formulas, and experimental errors are presented.

RESULTS AND DISCUSSION

Deactivation of Excited States in *Meso*-Aryl-Substituted Porphyrins and Their Chemical Dimers

The main spectral features observed when changing from **OE**P to the corresponding *meso*-derivatives are shown in Fig. 3, and may be summarized as follows. At 295 K the absorption and fluorescence Q(0,0)-bands for mono- and di *meso*-aryl-substituted **OEP** molecules are slightly red-shifted by $\Delta\lambda \sim$ 6 to 9 nm relative to that of the **OEP** molecule. The relative decrease of the Q(0,0)-band intensities both in fluorescence and absorption with

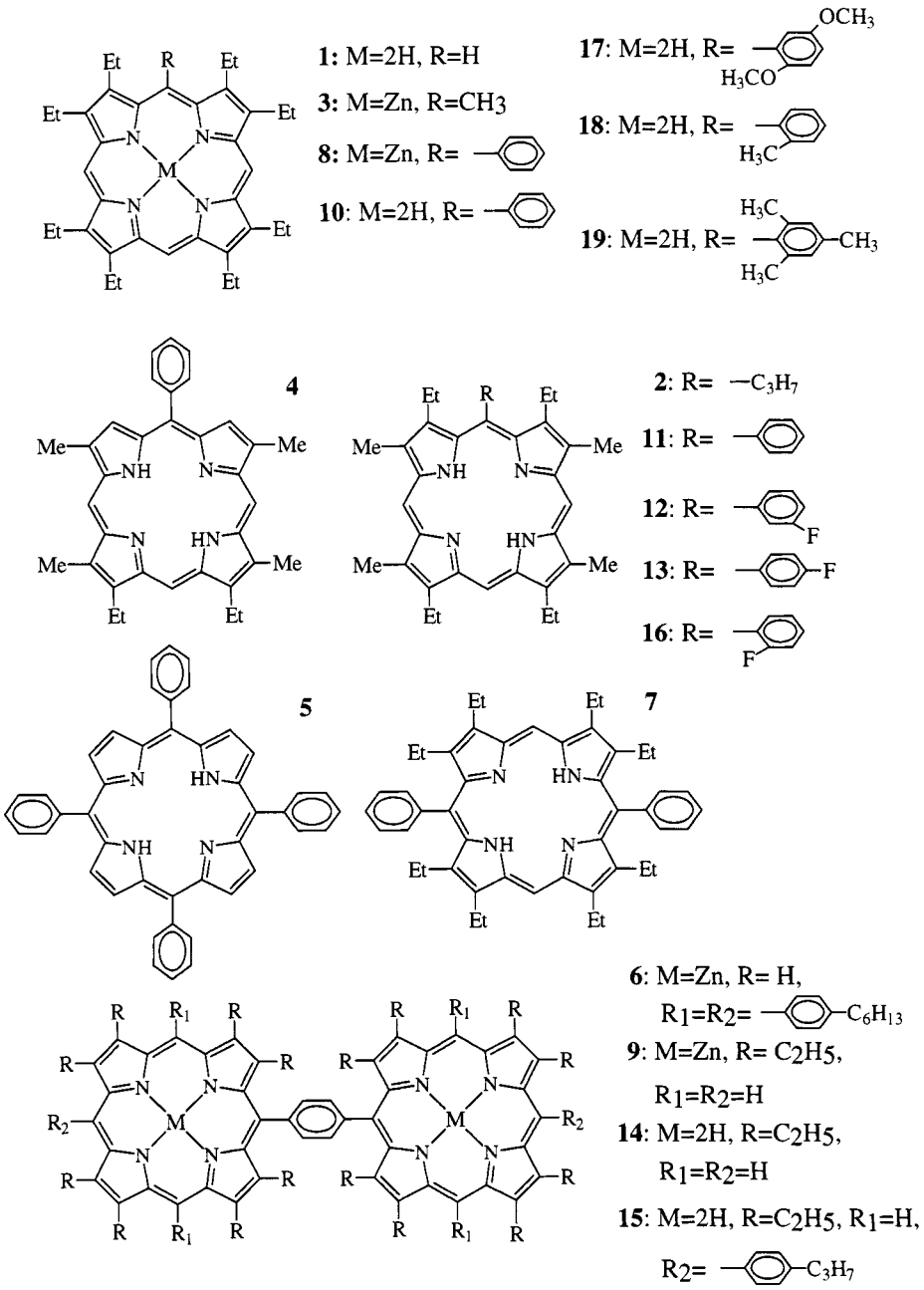

Fig. 1. Chemical structures of *meso*-aryl-substituted porphyrins and their dimers without NO_2 groups: **1**, OEP; **2**, EPII-Pr; **3**, ZnOEP-CH_3; **4**, TMDE-Ph; **5**, TPP; **6**, $(ZnHTPP)_2$; **7**, Ph-OEP-Ph; **8**, ZnOEP-Ph; **9**, $(ZnOEP)_2$-Ph; **10**, OEP-Ph; **11**, EPII-Ph; **12**, EPII-Ph(*m*-F); **13**, EPII-Ph(*p*-F); **14**, OEP-Ph-OEP; **15**, $(PrPh)_2$-$(OEP)_2$-Ph **16**, EPII-Ph(*o*-F); **17**, OEP-Ph$(OCH_3)_2$; **18**, OEP-Ph(*o*-CH_3); **19**, OEP-Ph$(CH_3)_3$.

respect to the corresponding intensities of vibronic Q(1,0)-bands is observed. Stokes shifts for **OEP** *meso*-aryl-substituted derivatives are 25 to 40 cm^{-1}. Upon a sequential transition from **OEP** to mono-, di-*meso*-phenyl-substituted porphyrins and then to the dimers, the phosphorescence emission at 77 K tends to be red-shifted with simultaneous transformation of the four-band spectrum to the two-band shape. These tendencies reflect the well-known spectro-structural correlation when changing from planar β-pyrrole-alkyl-substituted porphyrins [21] to structures that are close to planar tetraphenylporphyrin (**TPP**) [22]. In the sequential series of **OEP** → **OEP-Ph**

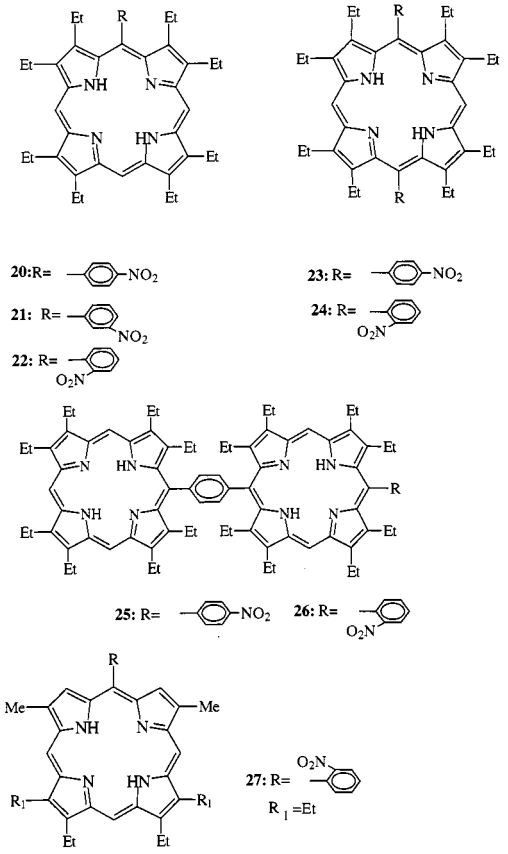

Fig. 2. Chemical structures of *meso*-nitro-phenyl-substituted porphyrins and their dimers: **20**, OEP-Ph(p-NO_2); **21**, OEP-Ph(m-NO_2); **22**, OEP-Ph(o-NO_2); **23**, (p-NO_2)Ph-OEP-Ph(p-NO_2); **24**, (o-NO_2)Ph-OEP-Ph(o-NO_2); **25**, OEP-Ph-OEP-Ph(p-NO_2); **26**, OEP-Ph-OEP-Ph(o-NO_2); **27**, TEDM-Ph(o-NO_2).

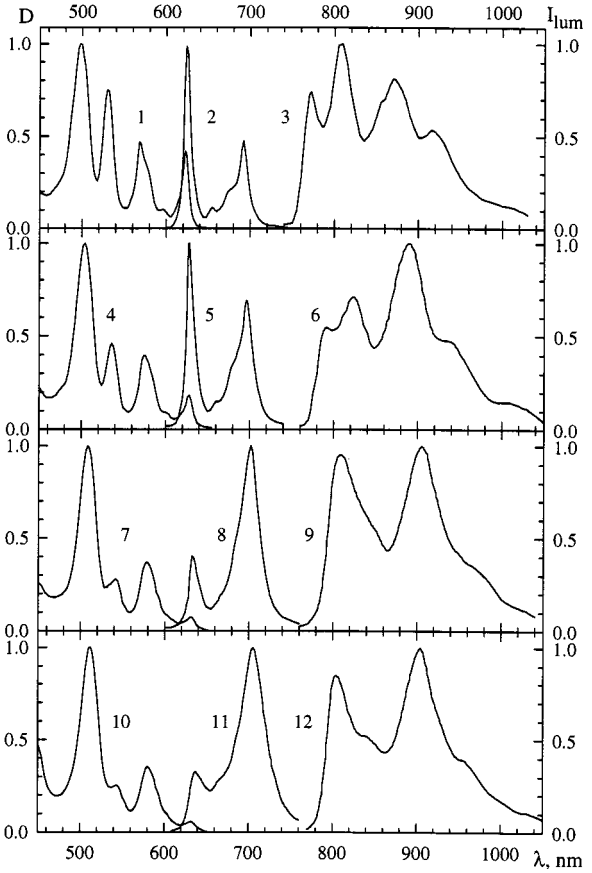

Fig. 3. Absorption (1, 4, 7, 10), fluorescence (2, 5, 8, 11) and phosphorescence (3, 6, 9, 12) spectra for porphyrins with mono- and di-*meso*-aryl substitution: **OEP** (1–3); **OEP-Ph** (4–6); **Ph-OEP-Ph** (7–9) and **$(PrPh)_2$-$(OEP)_2$-Ph** (10–12). Absorption and fluorescence were measured in toluene at 295 K; phosphorescence was registered in a glassy methylcyclohexane-toluene mixture (6:1) at 77 K.

→ **Ph-OEP-Ph**, the change of photophysical parameters at 295 K (Table I) reflects the well-documented monotonic decrease of fluorescence lifetimes (τ_S) and quantum yields (φ_F) upon transformation from **OEP** to the **TPP** molecule [21, 22]. At 77 K τ_S and φ_F values increase by ~35-40% for both OEP and its *meso*-phenyl-substituted derivatives. This is a typical behavior for planar porphyrins [23]. Finally, for the dimers, **OEP-Ph-OEP** and **$PrPh$-$(OEP)_2$-$PhPr$**, a small decrease of τ_S and φ_F is related to the manifestation of excitonic effects for various porphyrin chemical dimers with a small overlapping of π-conjugated macrocycles [15,16]. As a whole, all these spectral-energetic characteristics and tendencies indicate that for mono- and di-*meso*-aryl-substituted **OEP** molecules and their chemical dimers the conformational dynamics at 295 K, which results in the enhancement of the non-radiative deactivation of the S_1 states, does not take place.

In contrast to this, the data collected in Table I show evidently that some unusual effects are found for the T_1 state deactivation of **OEP** *meso*-phenyl derivatives at 295 K. The comparative examination of photophysical characteristics for the compounds taking into account their structural properties allows elucidation of the following main results. At 295 K in degassed toluene solutions, the changing from the **OEP** molecule (τ_T^0 = 1200 μs) to the mono- and di-*meso*-aryl-substituted **OEP** and **EPII** molecules, as well as to **OEP** chemical dimers with the phenyl spacer, leads to the shortening of τ_T^0 values by 300 to 500 times. The lifetime τ_T^0 = 4.0 μs for **OEP-Ph** is practically the same in toluene and glycerol and the T_1 state decay is monoexponential in both cases, but in an acrylic polymer film this value increases to 5000 μs. At 77 K in glassy rigid matrices the T_1 state lifetimes increase to tens of milliseconds for all compounds being investigated and the phosphores-

Table I. Photophysical and Photochemical Properties of *meso*-Aryl-Substituted Porphyrins and Their Chemical Dimers

Compound	τ_S (ns), 295 K	τ^0_S (ns), 295 K	φ_F, 295 K	$\varphi_P \times 10^4$, 77 K	τ_P/τ_T[a] (ms), 77 K	τ_T (ns), 295 K	τ^0_T (μs), 295 K	γ_T	γ_Δ
1. OEP	12.4	19.1	0.09	6.3	16/21[a]	330[b]	1200	0.80[b]	0.75[b]
2. EPII-Pr	—	—	—	—	—	260	1000	—	—
3. ZnOEP-CH_3	1.6	1.7	0.03	70	35/31[a]	360[b]	1200	1.0	0.85[b]
4. TMDE-Ph	11.3	17.1	0.06	1.8	16	265	1640	0.85	0.90
5. TPP	9.7	12.2	0.09	0.6	4.9/5.8[a]	400[b]	1000	0.82	0.68[b]
6. $(ZnHTPP)_2$	1.5	1.6	0.02	10	22.3/14.5[a]	605	1160	—	—
7. Ph-OEP-Ph	9.9	13.0	0.05	1.0	10.3/13.5[a]	380	16.5	—	—
8. ZnOEP-Ph	1.5	1.6	0.03	300	90/25[a]	355	5.8	—	—
9. $(ZnOEP)_2$-Ph	1.2	1.2	0.02	50	28.5/16.6[a]	925	2.85	—	—
10. OEP-Ph	11.2	16.0	0.05	1.9	14.5/11.1[a]	410	4.0	0.78	0.54
11. EPII-Ph	11.0	16.5	0.06	1.3	14.3	330	5.5	—	—
12. EPII-Ph(*m*-F)	10.7	15.9	0.07	1.8	14.5	390	4.2	—	—
13. EPII-Ph(*p*-F)	10.8	17.0	0.07	1.5	14.2	350	6.0	—	—
14. OEP-Ph-OEP	8.2	11.2	0.06	—	—	840	2.45	0.95	0.26
15. $(PrPh)_2$-$(OEP)_2$-Ph	7.9	10.6	0.05	1.2	10.2	900	3.6	—	0.45
16. EPII-Ph(*o*-F)	11.0	16.6	0.07	2.1	16.8	275	240	—	—
17. OEP-Ph$(OCH_3)_2$	11.2	16.7	0.07	2.1	16.3	330	125	—	—
18. OEP-Ph(*o*-CH_3)	—	—	0.07	1.8	14.7	370	1000	—	—
19. OEP-Ph$(CH_3)_3$	—	—	—	—	13.3	345	1490	—	—

[a] τ_T values were obtained from triplet-triplet absorption measurements in methylcyclohexane at 77 K, while phosphorescence τ_P values were measured in a glassy matrix of methylcyclohexane-toluene mixture (6:1) at 77 K.
[b] Data are cited from [24]. Meanings of all symbols are defined in the text.

cence quantum yield (φ_P) values are close to analogous values known for a planar **OEP** molecule. As can be seen from Table I, at 77 K τ_T, τ_P and φ_P values for all *meso*-phenyl substituted porphyrins being studied are close to the corresponding parameters obtained for **OEP**. This implies that the processes that lead to τ^0_T shortening for **OEP-Ph** type molecules in liquid solutions at 295 K are eliminated in rigid media.

At 295 K in degassed toluene solutions, the **TMDE-Ph** molecule, which has hydrogen atoms at the β-pyrrolic positions neighboring with the *meso*-phenyl (in contrast to ethyl groups in **OEP-Ph**), is characterized by the same long τ^0_T value as found for **OEP**. The analogous long τ^0_T lifetime is found for **EPII-Pr** molecule having the propyl group at the *meso*-position instead of the phenyl ring. It follows that the specific enhancement of the T_1 non-radiative quenching is characteristic for porphyrins having both the *meso*-phenyl and bulky substituents at the neighboring β-pyrrolic positions. On the other hand, as seen from Table I, in the case of **EPII-Ph(*o*-F)**, **OEP-Ph$(OCH_3)_2$**, **OEP-Ph(*o*-CH_3)** and **OEPPh$(CH_3)_3$** molecules having bulky substituents in *ortho*-position of the phenyl ring, the τ^0_T values increase to the ms time scale. However, the presence of a fluorine atom in *para*- or *meta*-position of the phenyl ring in **EPII-Ph(*p*-F)** and **EPII-Ph(*m*-F)** molecules does not lead to an increase of τ^0_T values relative to the short T_1 state lifetime of the **EPII-Ph** molecule. This interesting fact sheds light on the principal role of the bulky *ortho*-substituents in steric effects for **OEP-Ph** type molecules.

At room temperatures in degassed toluene, τ^0_T values for **Zn-OEP-Ph** and its chemical dimer are of the same order of magnitude as those for the corresponding porphyrin free bases. The deuteration of the two central iminohydrogens of **OEP-Ph** or the deuteration of non-substituted *meso*-positions in **Ph-OEP-Ph** hardly change their τ^0_T values. These facts indicate that the effective T_1 state quenching found for **OEP** *meso*-phenyl derivatives is not connected with the activation and enhancement of accepting high-frequency NH and CH modes of the porphyrin macrocycle [23].

Table I shows that at room temperature the corresponding τ^0_S and φ_F values for **OEP-Ph** and **EPII-Ph** type molecules are practically insensitive to the variation of substituents around the *meso*-phenyl ring. In addition, the probabilities of the radiative transition from the S_1 state (calculated on the basis of the Strickler-Berg formulae) do not vary for the compounds of the given group. It follows that the rate constants of the intersystem crossing $S_1 \sim\sim> T_1$ to the low lying excited T_1 state ($r \sim 4.0 \cdot 10^7$ s^{-1}) virtually do not vary upon changing from **OEP-Ph** to *meso*-phenyl-substituted analogs. We found that the

sequential change from **OEP** to **OEP-Ph** and then to the dimer, **OEP-Ph-OEP**, is not accompanied by decreasing intersystem crossing $S_1 \sim\sim> T_1$ quantum yields at 295 K in degassed toluene solutions. Nevertheless, the noticeable decrease of singlet oxygen generation quantum yields γ_Δ is observed for **OEP-Ph** and **OEP-Ph-OEP** at the same conditions. For the latter dimer compound the quantum efficiency of the singlet oxygen formation is estimated by the value of $\Gamma = \gamma_\Delta/\gamma_T \approx 0.3$ while for "normal" planar porphyrins $\Gamma \approx 1.0$ [24]. These facts indicate additionally that at 295 K the non-radiative deactivation for **OEP-Ph** type molecules is enhanced in T_1 states exclusively.

Taking into consideration all experimental facts presented above, we assumed that the strong decrease of τ_T^0 values for *meso*-phenyl-substituted **OEP** type molecules at 295 K may be determined by the internal motions (librations) and/or the possible overall tumbling of the phenyl ring around the single C-C bond and its interaction with a π-conjugated macrocycle. As a result of this, when the phenyl ring is coplanar with the sterically hindered porphyrin macrocycle in the excited triplet transition state, the non-planar deformations of the porphyrin skeleton may take place leading to the enhancement of the T_1 state non-radiative deactivation. In addition, it is evident that steric hindrances to *meso*-phenyl rotational motions by flanking bulky groups at the β-pyrrolic positions and corresponding substituents in ortho-position of the phenyl seem to play the essential role in the T_1 state non-radiative deactivation for porphyrins bearing *meso*-phenyls.

On the basis of this assumption and using the semiquantitative consideration of steric effects on the atropoisomerization in *ortho*-substituted tetraphenylporphyrins [25], we calculated the overlap geometrical parameters Σr*. These parameters are defined as the "apparent overlap" of flanking substituents at the β-pyrrolic positions of the porphyrin macrocycle with the corresponding groups attached in the *meso*-position of macrocycle or in the *ortho*-position of the phenyl ring when the porphyrin molecule is in the excited triplet transition state with a coplanar arrangement of the porphyrin and phenyl ring planes. According to the procedure described in [25], Σr* values for the compounds were calculated from projections in the hypothetical coplanar arrangement corresponding bond lengths of substituents in the porphyrin macrocycle (L_x, L_y) and in *ortho*-positions of the phenyl ring (l_x, l_y), intercenter distances (d_1, d_2) as well as the effective Van der Waals radii (r) for interacting substituents (Fig. 4). Chemical structures were calculated by quantum chemistry methods (HyperChem software, release 4, geometry optimization with semiempirical AM1 and PM3 methods).

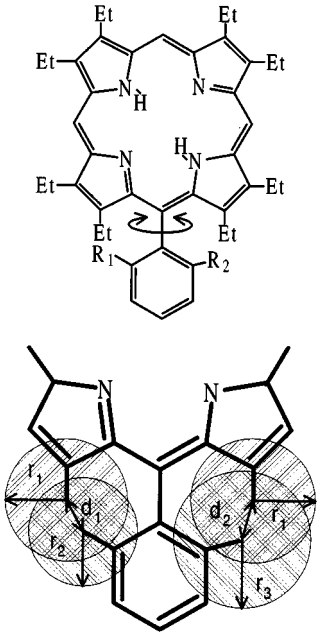

Fig. 4. Schematic structural presentation of the effective Van der Waals radii (r_w) for interacting substituents, intercenter distances (d_1, d_2) and corresponding substituent bond lengths in the porphyrin macrocycle and in *ortho*-positions of the phenyl ring (shown by solid lines) for the hypothetical coplanar arrangement of the porphyrin macrocycle and the phenyl ring planes (after HyperChem molecular modeling, HyperChem software, release 4, semiempirical AM1 and PM3 methods). Calculations of the overlap geometrical parameters Σr^* for every compound were carried out according to the expression [25]: $\Sigma r^* = (r^x_{w1} + r^x_{w2}) - d_x + (r^y_{w1} + r^y_{w2}) - d_y$, where indexes *x* and *y* correspond to parameters for left and right substituents.

The calculated Σr* values for the compounds under consideration were used to determine the correlative dependence, $\ln(k_T^0) = \ln(1/\tau_T^0) = f(\Sigma r^*)$, presented in Fig. 5. As shown, low $\ln(k_T^0)$ values (that is the absence or a small quenching of the T_1 state) are observed in the range of $\Sigma r^* < 3.4$ A^0 or $\Sigma r^* > 4.8$ A^0. For the first range, it is evident that librations of *meso*-substituents in the conditions of the partial overlap of Van der Waals spheres do not cause the essential non-planar distortions of the porphyrin macrocycle. For the second range, the overlap of Van der Waals spheres for the corresponding *ortho*-substituents in *meso*-phenyl and flanking substituents at the β-pyrrolic positions of the porphyrin macrocycle is so large that within T_1 state lifetimes ($\tau_T^0 \approx 1000$ μs) any rotations of the phenyl ring can not take place and its libration motions are even limited. The last conclusion is supported by the recent experimental results on the ^{13}C spin-lattice relaxation time of for *meso*-arylporphyrins having hydrogen atoms or methyl substituents at the β-pyrrolic positions adjacent to the phenyl rings [26]. Summing up all these facts one may conclude that for the

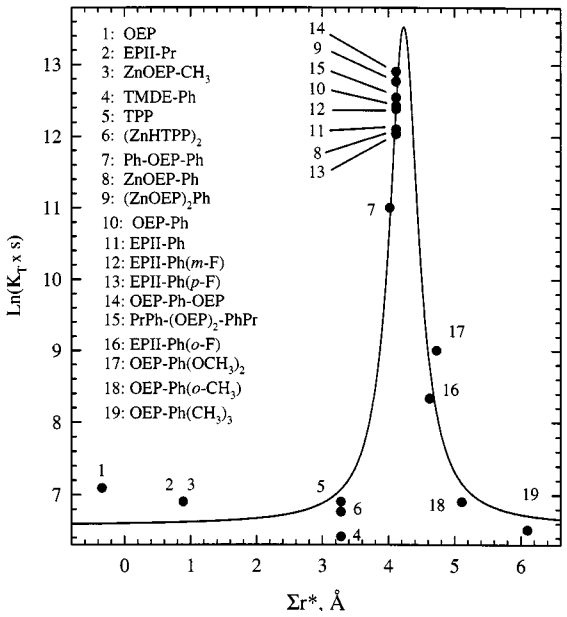

Fig. 5. The correlative dependence of the triplet state deactivation rate constants k_T^0 on the overlap geometrical parameter Σr^*, $1n(k_T^0) = 1n(1/\tau_T^0) = f(\Sigma r^*)$, for the compounds being studied in toluene at 295 K.

geometrical parameters $\Sigma r^* < 3.4$ A^0 or $\Sigma r^* > 4.8$ A^0 the porphyrin macrocycle is still planar in the T_1 state and the corresponding molecules are characterized by long τ_T^0 values without any essential enhancement of the T_1 state non-radiative deactivation.

High ln (k_T^0) values (that is the strong T_1 state non-radiative deactivation) in the middle range of 3.4 A^0 $< \Sigma r^* <$ 4.8 A^0 are presumed to be due to the fact that in this case torsion librations of the phenyl ring may lead to the non-planar deformations of the sterically hindered porphyrin macrocycle in the excited triplet state. Semiempirical calculations indicate that **OEP-Ph** type molecules in the T_1 state are characterized by the a-planar structure of the porphyrin macrocycle connected with the rotation of pyrrolic rings (flanking the *meso* phenyl substituent) around the C_α- C_α axis wherein nitrogen atoms and β-carbons of the pyrrolic ring are on opposite sides of the porphyrin plane. In addition, these calculations show [20] that in the hypothetical transient non-planar porphyrin conformation (where the *meso*-phenyl ring is coplanar with the porphyrin macrocycle) the energy gap between S_0 and T_1 levels $\Delta E(T_1 - S_0)$ is smaller than that for a planar conformation. Finally, our preliminary experiments showed that at 295 K in toluene the transient T-T absorption spectra for long-lived **OEP** and **OEP-Ph (*o*-CH$_3$)** molecules were practically the same while those for the short-living **OEP-Ph** molecule were characterized by different relative intensities and positions of their maxima. We believe that these spectral data indicate that the conformational state of the T_1 excited **OEP-Ph** molecule may be connected with a progressive distortion of the porphyrin macrocycle from the planarity, in contrast to that of planar **OEP** and **OEP-Ph (*o*-CH$_3$)** compounds.

At this point, one may advance some physical reasons leading to the enhancement of the dynamic non-radiative relaxation of T_1 excited states for mono- and di-*meso*-phenyl-substituted octaethylporphyrins in liquid solutions at 295 K. If we postulate that the decrease of the porphyrin skeleton rigidity in the excited T_1 state takes place, the libration motions of *meso*-phenyl ring with a high frequency around C-C bond may readily lead to a repeated progressive distortion of the porphyrin macrocycle from the planarity. Correspondingly, the decrease of $\Delta E(T_1 - S_0)$ values for the non-planar **OEP-Ph** type molecules must lead to an acceleration of the T_1 state non-radiative deactivation $T_1 \sim\sim> S_0$ due to the enhancement of the Franck-Condon factor [27]. Clearly, other reasons should be sought. The non-planar distortion of the porphyrin molecule in the T_1 state may lead to additional singlet and triplet state mixing facilitated by the enhancement of spin-orbit coupling due to the out-of-plane displacement of nitrogen atoms and the corresponding rise of one-center wavefunction overlap integrals involving the central nitrogen n-orbitals and porphyrin π-orbitals [28]. Finally, it is not excluded that in non-planar porphyrin conformations the enhancement of the T_1 state non-radiative deactivation may be caused by the initiation of some new types of accepting modes [29]. It is most reasonable to propose that all these factors may be the case for the systems of interest.

It should be mentioned that in steady-state phosphorescence spectra of **Pd-OEP-Ph** in toluene at 295 K (with a strongly shortened τ_T^0 value with respect to that for **Pd-OEP**) we have not found any new additional long-wavelength bands corresponding to the radiative $T_1 \rightarrow S_0$ deactivation of the non-planar porphyrin macrocycle. In addition, as we discussed above, τ_T^0 values for **OEP-Ph** coincide in toluene and glycerol at 295 K and the T_1 state decay is monoexponential in both cases. All these facts permit us to assume that the lifetime of the porphyrin non-planar conformation is very small compare to τ_T time scale and the distortion itself may be characterized as the dynamic reversible transformation.

Excited States Deactivation in *Meso*-Nitro-Phenyl-Substituted Porphyrins and Their Chemical Dimers

Steady-state measurements have shown that at 295 K absorption and fluorescence spectra of *para*- and *meta*-

nitro-substituted porphyrins remain practically the same relative to those for the corresponding *meso*-phenyl octaethylporphyrins without a NO_2 group. In the case of the *ortho*-NO_2 substitution the Stokes shift remains constant, but the electronic spectra are slightly red-shifted by $\Delta\lambda \sim 1$ to 6 nm. In addition, the relative decrease of the Q(0,0)-band intensities both in fluorescence and absorption spectra with respect to the corresponding intensities of vibronic Q(1,0)-bands is observed, as well as there being an increase in the halfwidth (by ~1.5 times) of the pure electronic transition bands. The same effects were observed for **TPP** containing *p*-benzoquinone in the *meso*-position [30] and were explained by the increased charge-transfer character of electronic states for the donor-acceptor complex. Spectral properties of the dimer **OEP-Ph-OEP** remain practically unchanged upon nitro substitution.

The experimental photophysical parameters for *meso*-nitro-substituted compounds at 295 K and 77 K are collected in Table II. Comparing these data with results presented in Table I for the corresponding molecules without the NO_2 group and taking into account structural properties of the compounds under consideration, the following findings may be summarized.

In degassed toluene solutions at 295 K, the presence of the NO_2 group in *para*- and *meta*-positions of the phenyl ring in the **OEP-Ph** molecule or in the **OEP-Ph-OEP** dimer influences the fluorescence quantum yields φ_F^0 and the lifetimes τ_S^0 weakly. A weak quenching of fluorescence with the rate constants of $k_{et}^S = 1.2\ 10^6 \div 1.0 \cdot 10^7 s^{-1}$ is detected, and this is smaller by at least one order of magnitude than the total rate constants of the S_1 state deactivation. Although the *para*-position of the phenyl ring is far from the porphyrin in comparison with the *meta*-position, minimal fluorescence quenching is observed for a *meta*-NO_2 substitution relative to that for the *para*-NO_2-substituted compounds. In addition, a noticeable decrease of T_1 state lifetimes τ_T^0 is found for *para*- and *meta*-NO_2-substituted porphyrins. So, for **OEP-Ph(*p*-NO_2)**, the τ_T^0 value is reduced by 2.1 times with respect to that for **OEP-Ph**. The existence of the second nitro-group in the **(*p*-NO_2)Ph-OEP-Ph(*p*-NO_2)** molecule leads to the enhancement of quenching up to 5.5 times, while for the dimer **OEP-Ph-OEP-Ph(*p*-NO_2)** the additional quenching of the T_1 state is not observed as compared to the τ_T^0 value for the initial dimer **OEP-Ph-OEP**. As in the case of S_1 states, the T_1 state quenching is more pronounced in *para*-NO_2-substituted **OEP-Ph(*p*-NO_2)** molecule than that in **OEP-Ph(*m*-NO_2)**.

For *ortho*-NO_2-substituted porphyrins and their dimers the fluorescence quenching is strongly enhanced. In toluene at 295 K, φ_F values are decreased by 12–25 times and the lifetimes τ_S^0 are shortened by ~100 times. Calculated from the τ_S measurements, the rate constant of S_1 quenching varies up to the value of $k_{et}^S = 9.5 \cdot 10^9\ s^{-1}$. Such strong fluorescence quenching for nitroporphyrins in non-polar solvents is reported here for the first time and it is significantly greater than that previously found for numerous covalently linked porphyrin-NO_2 systems in liquid non-polar solutions at room temperature [30–35], where k_{et}^S values were in the range of $(1 \div 5) \cdot 10^8\ s^{-1}$. In addition, in *ortho*-nitro-substituted porphy-

Table II. Photophysical and Photochemical Parameters of *meso*-Nitro-Phenyl-Substituted Porphyrins and Their Chemical Dimers in Toluene at 295 K and in a Glassy Matrix of Methylcyclohexane-Toluene Mixture (6:1) at 77 K

Compound	τ_S (ns), 295 K	$\tau^0{}_S$ (ns), 295 K	τ_S (ns), 77 K	φ_F, 295 K	φ_F, 77 K	$\varphi_P \times 10^4$, 77 K	τ_T (ms), 77 K	τ_T (ns), 295 K	$\tau^0{}_T$ (μs), 295 K	γ_T	γ_Δ	$k_S{}^b \times 10^9$ ($M^{-1}s^{-1}$)	$k_T{}^b \times 10^9$ ($M^{-1}s^{-1}$)	$k^o{}_{\pi}{}^c$ (s^{-1})	$k^T{}_q{}^c$ (s^{-1})
OEP-Ph(*p*-NO_2)	10.7	15.4	21.3	0.05	0.06	1.5	13.5	710	1.9	—	0.3	15.8	0.5	$4.4 \cdot 10^6$	$2.8 \cdot 10^5$
OEP-Ph(*m*-NO_2)	11.5	15.7	—	0.07	0.09	3.0	16.9	470	3.0	—	—	12.9	1.0	$1.2 \cdot 10^6$	$8.0 \cdot 10^4$
OEP-Ph(*o*-NO_2)	0.105[a]	0.105	20.2	0.002	0.06	1.4	13.0	700	0.75	~0.1	<0.01	—	—	$9.5 \cdot 10^9$	$1.3 \cdot 10^6$
(*p*-NO_2)Ph-OEP-Ph(*p*-NO_2)	10.5	12.6	—	0.07	0.08	2.3	10.1	690	3.0	0.65	0.55	9.0	0.6	$3.0 \cdot 10^6$	$2.7 \cdot 10^5$
(*o*-NO_2)Ph-OEP-Ph(*o*-No_2)	0.10[a]	0.10	16.0	0.001	0.07	1.6	11.0	400	0.5	~0.2	<0.01	—	0.3	$9.5 \cdot 10^9$	$2.0 \cdot 10^6$
OEP-Ph-OEP-Ph(*p*-NO_2)	7.8	10.1	15.0	0.04	0.07	1.7	8.2	865	2.4	—	0.3	15.8	0.4	$1.0 \cdot 10^7$	$<1 \cdot 10^5$
OEP-Ph-OEP-Ph(*o*-NO_2)	0.3	0.3	16.0	0.005	0.04	0.9	8.2	450	0.5	—	<0.01	—	—	$3.2 \cdot 10^9$	$1.6 \cdot 10^6$
TEDM-Ph(*o*-NO_2)	1.7	1.7	—	0.01	0.07	2.2	12.9	315	195	—	—	—	1.8	$5.0 \cdot 10^8$	$4.5 \cdot 10^3$

[a] Data were obtained using the picosecond spectrometer.

[b] Calculations of the second-order rate constants of S_1 and T_1 states quenching by molecular oxygen were done using the Stern-Volmer equation $\tau^0/\tau = 1 + kC\tau^0$, where $C = 1.8 \cdot 10^{-3}$M is O_2 concentration in toluene [33, 36, 44].

[c] Calculations of the rate constants of S_1 and T_1 states quenching were carried out on the base of measured lifetimes using the well-known formula $k = (1/\tau) - (1/\tau^0)$; in the case of triplet states quenching τ_T^0 values corresponding to unquenched T_1 rates were found using the correlative dependence $\ln(k_T^0) = \ln(1/\tau_T^0) = f(\Sigma r^*)$ for compounds without the *ortho*-NO_2 group but with the *ortho*-substituent characterized by the same overlap geometrical parameter Σr^* (Fig. 5).

rins and their dimers a pronounced enhancement of the T_1 quenching was also found. For instance, in degassed toluene solution at 295 K, for the dimer **(*o*-NO_2)Ph-OEP-Ph(*o*-No_2)** having two nitro-groups in the opposite *meso*-phenyls the τ_T^0 value is reduced by a factor of 33 relative to that for the dimer **OEP-Ph-OEP**.

Under the same experimental conditions, the comparison of data obtained for **TMDE-Ph** and **TEDM-Ph(*o*-NO_2)** molecules (both lacking bulky C_2H_5 substituents at the β-pyrrolic positions neighboring the phenyl ring) shows that the decrease of τ_S^0 and τ_T^0 lifetimes for NO_2-containing compound is comparatively smaller than that observed when changing from **OEP-Ph** to the **OEP-Ph(*o*-NO_2)** molecule. For instance, in **TEDM-Ph(*o*-NO_2)** the rate constant of S_1 quenching was found to be $k_{et}^S = 5.0 \cdot 10^{-8}\ s^{-1}$, which is ∼20 times smaller than the k_{et}^S value for **OEP-Ph(*o*-NO_2)**. The reason for this effect will be discussed below.

The additional non-radiative deactivation of the locally excited S_1 and T_1 states manifests itself in the interaction of *meso*-nitro-phenyl-substituted porphyrins and their dimers with molecular oxygen in toluene solutions at 295 K. As seen in Table II, in the case of *para*- and *meta*-nitro substitution the second-order rate constant of S_1 quenching by O_2 (k_S) does not depend practically on the position of the NO_2 group and is close to that for **OEP-Ph** ($k_s = 1.4 \cdot 10^{10}\ M^{-1}s^{-1}$), where it is close to the diffusion-limited k_S values known for planar porphyrins [33, 36]. Because of the strong S_1 quenching for *ortho*-NO_2-substituted compounds (down to ps lifetimes), the estimation of k_S values in this case seemed to be rather difficult at normal atmospheric pressure.

Our results show also that for all *meso*-nitro-phenyl-substituted porphyrins, the second-order rate constants of T_1 state quenching by molecular oxygen (k_T) in toluene at 295 K are decreased relative to those for the corresponding compounds without nitro-groups. For *meta*-NO_2-substituted porphyrins, the observed decrease is minimal. In the case of *para*-nitro substitution the decrease of k_T values by a factor of 1.5–2.5 is the smallest for the dimer **OEP-Ph-OEP-Ph(*p*-NO_2)**. At the same time, for the *ortho*-nitro-substituted compound, **(*o*-NO_2)Ph-OEP-Ph(*o*-NO_2)**, the k_T value is reduced by ∼5 times relative to $k_T = 1.35 \cdot 10^{10}\ M^{-1}s^{-1}$ for the **Ph-OEP-Ph** molecule. These results are consistent with the fact [36] that the rate constant of T_1 state quenching by molecular oxygen correlates with the tetrapyrrole macrocycle oxidation potential and decreases as the contribution of the charge transfer state in the collision complex [*porphyrin. . .oxygen*] decreases.

The T_1 quenching for *meso*-nitro-phenyl-substituted octaethylporphyrins manifests itself also in a noticeable decrease of quantum yields γ_Δ of singlet oxygen generation by these compounds. For instance, the γ_Δ value for **OEP-Ph(*p*-NO_2)** is reduced by a factor of 2 relative to that of **OEP-Ph**. For *ortho*-nitro-substituted compounds, the detection of the singlet oxygen emission at normal atmospheric conditions was almost impossible because of very efficient non-radiative T_1 deactivation.

Finally, it must be stressed that the quenching of the excited S_1 and T_1 states depends strongly on the polarity of the solvents being used (acetone, acetonitrile or dimetylformamide). For example, for the **OEP-Ph(*p*-NO_2)** molecule the fluorescence quantum yield is decreased to a value of $\varphi_F^0 = 0.015$ in acetone at 295 K, and, respectively, values of $\varphi_F^0 < 0.002$ and $\tau_S^0 \approx 20$ ps were obtained in dimetylformamide. The corresponding parameters $\varphi_F^0 < 0.001$ and $\tau_S^0 \approx 5$ ps were measured for **OEP-Ph(*o*-NO_2)** in pyridine-acetonitrile mixture (1:10). A noticeable but a smaller effect was detected for **OEP-Ph(*m*-NO_2)** in acetonitrile ($\varphi_F^0 = 0.003$ and $\tau_S^0 \approx 600$ ps). The maximal quenching is found for the **OEP-Ph(*p*-NO_2)** molecule as the solvent polarity increases. At the same time, in glassy matrices at 77 K the quenching of excited states is fully absent for all the systems under consideration.

As seen from the results presented above in Table I and discussed partly in [20], the *meso*-phenyl substitution in **OEP** type molecules and their chemical dimers with phenyl spacer does not lead to the additional non-radiative deactivation of S_1 states. Thus, the reasonable interpretation of the observed fluorescence quenching for *meso*-nitro-phenyl-substituted compounds may be connected with ET processes with the participation of the porphyrin macrocycle singlet excited states. The sensitivity of the fluorescence quenching to the solvent polarity is consistent with this interpretation. From the findings described above it follows that the quenching effect is minimal for *meta*-NO_2 substitution, though the NO_2 group in a *para*-position is farther from the porphyrin macrocycle. A similar tendency was observed in carotenoid-porphyrin diads, where the efficiency of the triplet-triplet energy transfer depends on the structure of the *ortho*-, *meta*- and *para*-carotenoporphyrin isomers [37]. In according with arguments based on Huckel MO theory and discussed in [37], for the *meso*-phenyl substituents the orbital electronic densities of both HOMO's and LUMO's are higher for *ortho*- and *para*-positions than for *meta*-position. If this is the case for nitroporphyrins with the phenyl spacer, the smaller quenching effect for the *meta*-NO_2 substitution (or the minimal value of the ET rate constant k_{et}^S for the **OEP-Ph(*m*-NO_2)** molecule) with respect to that for the *para*-NO_2 may be explained by a smaller value of the electronic coupling between the electronic wavefunctions of the reactant and product

states with the participation of the bridge sites in the ET reactions [38]. In this relation, we suggest that in the **OEP-Ph(*m*-NO$_2$)** and *OEP-Ph(**p**-NO$_2$)* molecules as well as in the compounds with the same substitution, ET processes are affected by the linkage between donor and acceptor and realised with the participation of the *meso*-phenyl molecular orbitals (the so-called through-bond superexchange ET mechanism [37, 39]).

The highest values of the ET rate constants ($k_{et}^S = 9{,}5 \cdot 10^9$ s^{-1}) are determined for monomeric molecules with the *ortho*-NO_2 substitution. In this case the quantum yield of the singlet excited radical ion pair $^1[porphyrin^+ \ldots NO_2^-]$ formation is estimated to be $\varphi_{et}^S = 0.99$. One may conclude that for all compounds with *ortho*-NO_2 substitution the steric interactions of bulky substituents in β-positions of pyrrole rings with the NO_2 containing phenyl ring is favorable for the overlapping of interacting subunits (porphyrin macrocycle and NO_2 group). It leads to the effective quenching of porphyrin fluorescence via direct ET from the locally excited S_1 state to the low lying charge transfer (CT) state (the so-called through-space ET mechanism [39]). For the dimer **OEP-Ph-OEP-Ph(*o*-NO$_2$)** the ET rate constant k_{et}^S is reduced to one third of that for the corresponding monomer **OEP-Ph(*o*-NO$_2$)**. This reduction may be explained by the existence of the non-radiative S-S energy transfer between covalently linked porphyrin macrocycles (with the rate constant of $F^{SS} = (1.9 - 5.0) \cdot 10^9$ s^{-1} [40]) competing with ET processes. In its turn, the smaller fluorescence quenching for **TEDM-Ph(*o*-NO$_2$)** than that for **OEP-Ph(*o*-NO$_2$)** may be explained as follows. It is seen from Fig. 2 that the **TEDM-Ph(*o*-NO$_2$)** molecule does not have bulky C_2H_5 substituents at the β-pyrrolic positions neighboring the phenyl ring with an NO_2 group in the *ortho*-position. In this case, the overlap of the Van der Waals spheres for the corresponding *ortho*-substituents in *meso*-phenyl and flanking substituents at the β-pyrrolic positions of the porphyrin macrocycle is reduced relative to that for **OEP-Ph(*o*-NO$_2$)**. This means that for **TEDM-Ph(*o*-NO$_2$)** the amplitude of the *meso*-phenyl libration motions around C-C bond is larger than that for **OEP-Ph(*o*-NO$_2$)**. As a result, this leads to a reduced overlap of the porphyrin macrocycle and NO_2 group orbitals. Thus, the electronic coupling term for ET processes becomes smaller in the **TEDM-Ph(*o*-NO$_2$)** case. In this respect, inefficient ET in the **TPP** molecule containing a NO_2 group in the *ortho*-position of the phenyl ring [30] may be explained by the same reason. It is interesting to note that the ET rate constant $k_{et}^S = 5.0 \cdot 10^8$ s^{-1} for the **TEDM-Ph(*o*-NO$_2$)** molecule (Table II) is still higher than that for **TPP(*o*-NO$_2$)** ($k_{et}^S = 1.5 \cdot 10^8$ s^{-1} [30]) under the same conditions. The reason for this will be discussed in the next section.

Electron Transfer Processes in Nitroporphyrins

It is supposed that the high values which are obtained for the ET rate constants k_{et}^S for the *ortho*-NO_2 substituted octaethylporphyrins and their chemical dimers in toluene at 295 K can result from the fact that the introduction of bulky C_2H_5 groups at the β-pyrrolic positions flanking *ortho*-NO_2 *meso*-phenyl substituents on the porphyrin macrocycle leads to a considerable steric hindrance to librational motions of the phenyl ring around the single C-C bond joining it to the macrocycle. In fact, for steric reasons [41] and on the basis of our data on the optimized molecular structure models for **OEP-Ph(*o*-NO$_2$)** the phenyl plane is perpendicular to the plane of the tetrapyrrole macrocycle and the plane of the NO_2 group is perpendicular to the phenyl plane. Such geometry of the donor-acceptor pair provides the close overlap of molecular orbitals for interacting subunits what is favorable for the efficient electron transfer.

In condensed phase for the systems under consideration the hypothetical CT state energies may be properly calculated based on the formula [2,38,39]

$$E_{CT} = e(E_{1/2}^{ox} - E_{1/2}^{red}) - W \qquad (1)$$

where $E_{1/2}^{ox}$ is the one-electron oxidation potential of the donor (D), $E_{1/2}^{red}$ is the one-electron reduction potential of the acceptor (A), $W = e^2/4\pi\varepsilon_0\varepsilon_{st}r_{DA}$ is the Coulombic interaction energy between the ions at the distance r_{DA} in *D-A* pair, ε_0 is the dielectric perceptivity of free space, and ε_{st} is the static dielectric constant of the solvent. This estimation may be done only in highly polar media, where the energy *W* between strongly solvated ions is small.

Taking into account the estimations of the *W* value for porphyrins in acetonitrile (the static dielectric constant $\varepsilon_{st} = 35.9$) [42] as well as the intercenter distance r = 5.7 A° between the porphyrin and the *ortho*-NO_2 group (found for the optimized **OEP-Ph(*o*-NO$_2$)** structure), we determined a value of $W \approx 0.08$ eV. Accordingly, on the basis of known values of redox potentials for **OEP** ($E_{1/2}^{ox} = 0.81$ eV [43]), **TPP** ($E_{1/2}^{ox} = 1.08$ eV [44]) and nitro-benzene ($E_{1/2}^{red} = -1.08$ eV [44]) measured against calomel electrode in dimethylformamide ($\varepsilon = 36.7$), we estimated the CT state energies for **OEP-Ph(*o*-NO$_2$)** $E_{CT} = 1.8$ eV (14500 cm^{-1}) and **TPP(*o*-NO$_2$)** $E_{CT} = 2.1$ eV (16900 cm^{-1}). From these estimates, two principally different features of the energetics for these two molecules can be noted. First, for **TPP(*o*-NO$_2$)** the predicted CT state of the singlet excited radical ion pair is energetically higher by ~0.18 eV (1440 cm^{-1}) than the locally

excited S_1 state (E_{s1} = 15460 cm^{-1} or 1.92 eV on the basis of spectral data presented in [30]). Accordingly, the non-radiative deactivation of the S_1 state for the **TPP(*o*-NO$_2$)** molecule in liquid solutions at 295 K may be realised only through thermal population of the radical-ion pair state or due to increasing the rate constant of the non-radiative transition caused by the perturbation of its locally excited S_1 state by mixing with high-lying CT states [1, 45]. Secondly, in the case of **OEP-Ph(*o*-NO$_2$)** the predicted energy of the CT state is lower by ~0.17 eV (1370 cm^{-1}) than the energy of the excited S_1 state (E_{s1} = 15870 cm^{-1} or 1.97 eV, as determined from absorption and fluorescence spectra in dimethylforamide). Correspondingly, in this case one might expect that the additional deactivation of the porphyrin S_1 state will occur due to the direct population of the low-lying CT state with a high efficiency. Correspondingly, the difference in the ET rate constants for **TPP(*o*-NO$_2$)** and **TEDM-Ph(*o*-NO$_2$)** becomes clear. In fact, with the same steric factors resulting in similar values of the electronic coupling terms and due to the difference in the oxidation potentials of these compounds the hypothetical CT state energy in **TEDM-Ph(*o*-NO$_2$)** has to be lower than that of **TPP(*o*-NO$_2$)**. The lowering of the CT state energy for **TEDM-Ph(*o*-NO$_2$)** relative to that for **TPP(*o*-NO$_2$)** may lead to the enhancement of non-radiative reactivation of S_1 state in the former compound.

According to Marcus theory [39], at high temperatures the rate constant k_{et}^S for non-adiabatic electron transfer occurring within the "normal" region is given by the well-known relationships:

$$k_{et}^S = \frac{2\pi}{\hbar} \cdot \frac{V^2}{(4\pi\lambda k_B T)^{1/2}} \cdot \exp\left(-\frac{\Delta G^*}{k_B T}\right) \qquad (2)$$

$$\Delta G^* = \frac{(\Delta G^0 + \lambda)^2}{4\lambda} \qquad (3)$$

where T is the temperature, $\hbar$ is Plank's constant, V is the electronic coupling term between the electronic wavefunctions of the reactant and product states, k_B is Boltzman's constant, $\lambda = \lambda_{in} + \lambda_{solv}$ is the Gibbs reorganization energy, ΔG^0 is the standard Gibbs energy of the ET reaction, and ΔG^* is the Marcus-Gibbs activation energy. The reorganization energy λ is determined by the nuclear λ_{in} and solvent λ_{solv} reorganization energies. The reorganization energy λ_{in} arises from changes of the internal geometry and it is solvent independent. For porphyrin-acceptor systems without substantial geometry changes upon one-electron redox events, $\lambda_{in} \approx 0.2$ eV [2, 38, 46]. The external reorganization energy λ_{solv} depends essentially on the nature of solvent [39] and it is often calculated on the basis of the model that the donor and acceptor occupy hollow spheres of radii r_D and r_A, respectively, in dielectric continuum, with the distance r_{DA} between them [46]:

$$\lambda_{solv} = \frac{e^2}{4\pi\varepsilon_0}\left[\frac{1}{2r_D} + \frac{1}{2r_A} - \frac{1}{r_{DA}}\right]\left[\frac{1}{\varepsilon_{op}} - \frac{1}{\varepsilon_{st}}\right] \qquad (4)$$

where e is the charge transferred, $\varepsilon_{op} = n^2$ is the optical dielectric constant, and n is the refractive index.. For the systems under consideration we used the following parameters: r_D = 5 A^0 [2, 38], r_A = 3.5 A^0 and r_{DA} = 5.7 A^0 (based on the results of calculated optimized **OEP-Ph(*o*-NO$_2$)** structure). The values of the external reorganization energy λ_{solv} = 0.5 eV and the total reorganization energy λ = 0.7 eV were estimated in acetonitrile.

For ET from the locally excited singlet state of **OEP-Ph(*o*-NO$_2$)** molecule the standard Gibbs energy is calculated with the formula [47]

$$\Delta G^0 = e(E_{1/2}^{ox} - E_{1/2}^{red}) - W - E_{S1} \qquad (5)$$

The corresponding value is equal to $\Delta G^0 = -0.16$ eV in our case. As follows from these calculations $|\Delta G^0| < \lambda$ in the considered donor-acceptor pair, and the electron transfer in this case may be assigned to the "normal" region of the Marcus parabolic dependence, $\log k_{et}^S = f(-\Delta G^0)$. Finally, the Marcus Gibbs activation energy is estimated to be $\Delta G^* = 0.1$ eV.

As mentioned above, in polar solvents at 295 K the fluorescence quenching becomes stronger for all nitroporphyrins. In the framework of the semiclassical Marcus theory [39], the quenching enhancement may be connected with the lowering of the CT state energy and the reduction of the activation enthalpy ΔG^* with the concurrent increase of the standard Gibbs energy ΔG^0. On the basis of the picosecond transient spectroscopy data for **OEP-Ph(*o*-NO$_2$)** in dimethylformamide at 295 K ($\tau_s^0 \approx 5$ ps) the ET rate constant was estimated to be $k_{et}^S \approx 2 \cdot 10^{11}$ s^{-1}. Accordingly, it immediately follows from expression (2) and the parameters λ, ΔG^* and k_{et}^s obtained, that for **OEP-Ph(*o*-NO$_2$)** the electronic coupling matrix element V is ~190 cm^{-1} in dimethylformamide at room temperature.

On the other hand, ET reactions are non-adiabatic by Landau-Zener criteria if they satisfy the following relationship [47]

$$4\pi^2 V^2/h\omega(2\lambda k_B T)^{1/2} < 1 \qquad (6)$$

where ω is the characteristic frequency of the medium. At 300 K for typical low-frequency motions, ω = ~100 cm^{-1}. It is evident from this equation that for the found λ = 0.7 eV, the electronic coupling matrix element V must be <133 cm^{-1}, which does not differ essentially

from the estimate based on equation (2). Therefore we tend to believe that that at room temperature in polar media the fluorescence quenching of **OEP-Ph(*o*-NO_2)** may be referred to the limiting case of non-adiabatic ET with the possible manifestation of adiabatic effects in strongly polar solvents. If the ET process seems to be adiabatic with $V > 100$ cm^{-1}, it is possible to use the adiabaticity parameter of Rips and Jortner [48] in order to evaluate a possible influence of solvent dynamics on the electron transfer rate:

$$K = 4\pi V^2 \tau_L/\hbar\lambda \qquad (7)$$

where τ_L is the longitudinal relaxation time of the solvent (0.4 ps for dimethylformamide). Taking the corresponding parameters for **OEP-Ph(*o*-NO_2)** in dimethylformamide at 295 K, we find $K = 7$. In according with [49], the ET process is probably solvent controlled in this case. It means [50, 51] that the intrinsic ET rate becomes comparable with the time required for solvent molecules to reorient, and the observed ET rate may be determined primarily by solvent dynamics. However, for **OEP-Ph(*o*-NO_2)** in non-polar media (toluene) as well as for **OEP-Ph(*p*-NO_2)** and **OEP-Ph(*m*-NO_2)** molecules both in polar and non-polar solvents ET is essentially non-adiabatic.

Finally, within this framework we will discuss the formation and quenching of T_1 states for the *meso*-nitro substituted compounds in degassed toluene solutions at 295 K. It should be mentioned that for *para*- and *meta*-NO_2-substituted **OEP** molecules the determination of T_1 state quenching rate constants k_q^T using the equation $k_q^T = (1/\tau_T) - (1/\tau_T^0)$ was done in the usual way because of the absence of steric hindrance effects. However, for *ortho*-NO_2-containing compounds, steric interactions of C_2H_5 groups at the β-pyrrolic positions flanking bulky *ortho*-NO_2 substituents in the phenyl ring lead to libration motions and rotations of the phenyl ring to be more strongly hindered than in similar systems without the flanking ethyl groups. Therefore, for **such certainly** more conformationally constrained systems τ_T^0 values corresponding to unquenched T_1 states were found using the correlative dependence $\ln(k_T^0) = \ln(1/\tau_T^0) = f(\Sigma r^*)$ in Fig. 5 for corresponding compounds without an *ortho*-NO_2 group, but having an *ortho*-substituent with the same overlap geometrical parameter $\Sigma r^* = 5.11$ A^0.

Experimental data presented in Table II show that T_1 state quenching rate constants k_q^T are lower by 3–4 orders of magnitude than the corresponding k_{et}^S of S_1 state quenching. This result can not be explained within the semiclassical Marcus theory [2, 39, 47] for direct ET with the participation of triplet states. On the basis of our phosphorescence spectra for the compounds of interest at 77 K [49] we have estimated the T_1 energy for **OEP-Ph(*o*-NO_2)** to be $E_T = 1.56$ eV $= 12550$ cm^{-1}. Accordingly, the excited singlet CT state of the radical-ion pair ^{1}[*porphyrin*$^+$ . . . NO_2^-] lies above the locally excited T_1 state by ~0.24 eV (Fig. 6). In addition, we found that the temperature dependence of the T_1 quenching rate constant k_q^T for **OEP-Ph(*o*-NO_2)** in the toluene-acetone (3:1) mixture is the Arrhenius type with the activation energy value of $\Delta E_a = 0.21$ eV. This experimental value is in a good agreement with the above theoretical estimation. We conclude therefore that the T_1 state quenching is not due to direct ET from the triplet state.

In the **OEP-Ph(*o*-NO_2)** molecule the steric interactions of C_2H_5 groups at the β-pyrrolic positions flanking bulky *ortho*-NO_2 substituents in the phenyl ring will cause the libration motion of the phenyl ring around the single C-C bond to be strongly hindered. Because of this, the geometry of the donor-acceptor pair seems to be not flexible. Thus, the spin-exchange energy in this case is negligible and the spin rephasing between the singlet and triplet radical-ion pairs is rather fast with the corresponding rate constants of $k_{13} \approx k_{31} \approx 5.0 \cdot 10^7$ s^{-1} [50] (see Fig. 6). As follows from the photophysical parameters obtained for **OEP-Ph** (see Table I) the rate constant of the intersystem crossing from the singlet to the triplet state $S_1 \rightarrow T_1$ is estimated to be $r = 5.0 \cdot 10^7$ s^{-1}. Since in **OEP-Ph(*o*-NO_2)** the ET rate constant $k_{et}^S = 9.5 \cdot 10^9$ s$^{-1} >> r$, the direct population of the locally excited T_1 state has low probability for this compound. Thus, the

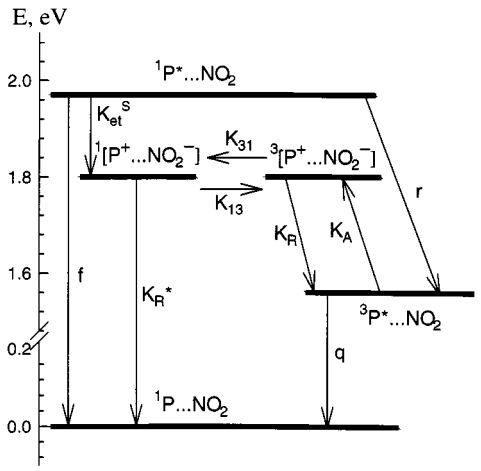

Fig. 6. Schematic energy diagram showing the energy levels and decay pathways of **OEP-Ph(*o*-NO_2)** in acetonitrile at 295 K. The rate constants are as follows: *f*, fluorescence; *r*, intersystem crossing from the singlet to the triplet state, $S_1 \rightsquigarrow T_1$; *q*, non-radiative intersystem crossing to the ground state, $T_1 \rightsquigarrow S_0$; k_R^*, charge recombination from the singlet radical ion pair; k_R, charge recombination from the triplet radical ion pair; k_{et}^S, electron transfer from the singlet state; k_{13} and k_{31}, spin rephasing between the singlet and triplet radical ion pairs; k_A, the thermally activated population of the triplet radical ion pair.

population of the locally excited T_1 state in this case may take place from the triplet radical-ion pair state $^3[OEP^+ \ldots NO_2^-]$ or directly from the singlet radical-ion pair state $^1[OEP^+ \ldots NO_2^-]$. This reasonable assumption is consistent with the fact that going from **OEP-Ph** to **OEP-Ph(*o*-NO_2)** in toluene at 295 K the decrease of the fluorescence quantum yield ($\varphi_F^0/\varphi_F \approx 25$) is not parallel with the intersystem crossing quantum yield ($\gamma_T^0/\gamma_T \approx 8$). Therefore, we conclude that at room temperature the non-radiative deactivation of the locally excited T_1 state in **OEP-Ph(*o*-NO_2)** may be realised via the thermal activation of the triplet and singlet states of the radical-ion pair followed by the charge recombination from these states to the ground state

$$(T_1)\ [^3P \ldots NO_2] \underset{K_R}{\overset{K^A}{\rightleftarrows}} {}^3[P^+ \ldots NO_2^-] \qquad (8)$$

$$\underset{K_{13}}{\overset{K_{31}}{\rightleftarrows}} {}^1[P^+ \ldots NO_2^-] \overset{K^R}{\rightarrow} [P \ldots NO_2]\ (S_0)$$

The corresponding rate constants are presented in Fig. 6. In this relation, it is impossible to exclude that the shortening of τ_T in **OEP-Ph(*o*-NO_2)** may also be caused by the increase of the intersystem crossing $T_1 \rightarrow S_0$ rate constant due to the perturbation of the excited T_1 state by mixing with upper-lying CT states of the radical-ion pair [45]. The detailed analysis of the temperature, polarity and viscosity influence on the T_1 state deactivation for *meso*-nitro-phenyl-substituted octaehylporphyrins and their dimers is in progress.

CONCLUSIONS

The results presented show that for *meso*-phenyl-substituted porphyrins and their chemical dimers with the phenyl spacer the steric interactions lead to the dynamic non-planarity of the porphyrin macrocycle in the excited triplet state. We have demonstrated for the first time a large decrease of triplet lifetimes (by $\sim 300 + 500$ times at 295 K in degassed toluene solutions) for mono- and di-*meso*-phenyl-containing porphyrins, their corresponding Zn- and Pd-complexes and their dimers having bulky substituents at the β-pyrrolic positions flanking *meso*-phenyl rings, while spectral-kinetic parameters of the S_0 and S_1 states remain unchanged. This quenching is explained by internal librations and a possible overall tumbling of the phenyl ring around the single C-C bond and its interaction with the π-conjugated macrocycle leading to non-planar dynamic distorted conformations that are realized exclusively in excited T_1-states.

Based on the above results we carried out a comprehensive investigation of the photophysical properties of *meso*-nitro-phenyl derivatives of **OEP** and their chemical dimers having covalently linked electron-accepting NO_2-groups in *para*-, *meta*- and *ortho*-positions of the phenyl ring. Our experimental findings and theoretical estimates have shown that steric interactions and the π-electron density distribution of the linkage between D and A play an essential role in the efficiency and the mechanism of photoinduced ET. The strong fluorescence quenching observed for *ortho*-NO_2 substituted compounds in the absence of the phenyl ring librations around a single C-C bond is caused by the intramolecular electron transfer from S_1 state of the porphyrin macrocycle (the normal region, a non-adiabatic case presumably, $V \approx 130/190$ cm^{-1} in dimethylformamide). The shortening of the T_1 state lifetimes observed for the same compounds in degassed toluene solutions at 295 K is explained by thermally activated transitions to upper-lying CT states of the radical-ion pair as well as by an increase of the $T_1 \sim\sim> S_0$ intersystem crossing rates as a result of mixing of T_1 and CT states.

The pronounced S_1 state quenching of porphyrins in non-polar solvents was observed for the first time and it is significantly greater than that found before for numerous covalently-linked porphyrin-NO_2 systems under the same conditions.

ACKNOWLEDGMENTS

Financial support from the National Foundation for Basic Research of Belarus (Grant No. Ph 96-92) is gratefully acknowledged. We thank Dr. S. Tikhomirov for providing us with the picosecond transient absorption measurements of S_1 state decays. We thank also Mr. D. Starukhin for his assistance in the temperature experiments on the T_1 state deactivation.

REFERENCES

1. V. Balzani and F. Scandola (1991) *Supramolecular Photochemistry*, Ellis Horwoord, New York/London/Toronto/Sydney/Tokyo/Singapore, pp. 161–196.
2. M. R. Wasielewski (1992) *Chem. Rev.* **92**, 435–461.
3. A Osuka et al. (1996) *J. Am. Chem. Soc.* **118**, 155–168.
4. D. Kuciauskas et al. (1997) *J. Phys. Chem. B* **101**, 429–440.
5. J. L. Sessler, B. Wang, and A. Harriman (1995) *J. Am. Chem. Soc.* **117**, 704–714.
6. M. O. Senge (1992) *J. Photochem. Photobiol.* **16**, 3–36.
7. K. M. Barkigia et al. (1990) *J. Am. Chem. Soc.* **112**, 8851–8857.
8. M. O. Senge and W. W. Kalish (1997) *Inorg. Chem.* **36**, 6103–6116.
9. K. M. Barkigia et al. (1998) *J. Phys. Chem.* **102**, 322–326.

10. P. Charlesworth et al. (1994) *J. Chem. Soc. Faraday Trans.* **90**, 1073–1076.
11. A. M. Shulga and G. V. Ponomarev (1984) *Khim. Geterotzikl. Soedinenii* 922–927 (in Russian).
12. A. M. Shulga and G. P. Gurinovich (1981) *Doklady Acad. Nauk BSSR* **25**, 55–58 (in Russian).
13. M. J. Gunter and L. N. Mander (1981) *J. Org. Chem.* **46**, 4792–4795.
14. R. Young and C. K. Chang (1985) *J. Am. Chem. Soc.* **107**, 898–909.
15. A. V. Chernook, A. M. Shulga, E. I. Zenkevich, U. Rempel, and Ch. von Borczyskowski (1996) *J. Phys. Chem.* **100**, 1918–1926.
16. J. L. Sessler, V. L. Capuno, and A. Harriman (1993) *J. Am. Chem. Soc.* **115**, 4618–4628.
17. A. Osuka et al. (1996) *J. Chem. Soc. Perkin Trans.* **2**, 199–203.
18. E. I. Zenkevich et al. (1996) *J. Photochem. Photobiol. B Biol.* **33**, 171–180.
19. S. M. Bachilo (1995) *J. Photochem. Photobiol. A Chem.* **91**, 111–115.
20. V. N. Knyukshto et al. (1998) *J. Appl. Spectr.* **65**, 471–475 (in Russian).
21. K. N. Solov'ev, V. N. Knyukshto, and M. P. Tzvirko (1976) *Opt. Spectrosc.* **41**, 964–970 (in Russian).
22. G. D. Egorova et al. (1980) *Opt. Spectrosc.* **48**, 1101–1109 (in Russian).
23. A. T. Gradyushko et al. (1978) *Opt. Spectrosc.* **44**, 458–464 (in Russian).
24. E. I. Sagun et al. (1991) *Khim. Phys.* **10**, 477–484 (in Russian).
25. M. J. Crossley et al. (1987) *J. Am. Chem. Soc.* **109**, 341–348.
26. L. Noss et al. (1997) *J. Phys. Chem.* **101**, 458–465.
27. N. Turro (1978) *Modern Molecular Phtochemistry*, Benjamin/Cummings, Menlo Park, CA, pp. 153–198.
28. M. K. Bowman (1977) *Chem. Phys. Lett.* **48**, 17–21.
29. S. L. Madey, S. Okajima, and E. C. Lim (1976) *J. Chem. Phys.* **65**, 1219–1220.
30. A. Harriman and R. J. Hosie (1981) *J. Chem. Soc. Faraday Trans.* **2**, 77, 1695–1702.
31. S. S. Dvornikov et al. (1986) *Opt. Spectrosc.* **61**, 1228–1234 (in Russian).
32. S. S. Dvornikov et al. (1987) *Opt. Spectrosc.* **63**, 1179–1181 (in Russian).
33. V. A. Ganzha et al. (1989) *J. Appli. Spectrosc.* **50**, 618–623 (in Russian).
34. D. Gust et al. (1990) *Photochem. Photobiol.* **51**, 419–426.
35. I. K. Shushkevich et al (1987). *J. Applied Spectrosc.* **46**, 538–587 (in Russian).
36. B. M. Dzhagarov et al. (1987) *Khim. Phys.* **6**, 919–928 (in Russian).
37. D. Gust et al. (1992) *J. Am. Chem. Soc.* **114**, 3590–3603.
38. W. B. Davis et al. (1997) *J. Phys. Chem.* **101**, 6158–6164.
39. P. Siddarth and R. A. Marcus (1993) *J. Phys. Chem.* **97**, 6111–6118.
40. E. I. Zenkevich et al. (1995) *Proc. Ind. Acad. Sci. (Chem. Sci.)* **107**, 795–802.
41. H. Sheer and J. J. Katz (1975) in K. M. Smith (Ed.), *Porphyrins and Metaloporphyrins*, Elsevier Scientific, Amsterdam–New York–Oxford, pp. 399–524.
42. N. Barboy and J. Feitelson (1984) *J. Phys. Chem.* **88**, 1065–1068.
43. J. Fuhrhop, K. Kadish, and D. Davis (1973) *J. Am. Chem. Soc.* **95**, 40–51.
44. S. L. Murrov, I. Carmichael, and G. L. Hug (1993) *Handbook of Photochemistry*, Marcel Dekker, New York–Basel–Hong Kong, pp. 269–278.
45. M. R. Wasielewski et al. (1990) *J. Am. Chem. Soc.* **112**, 6482–6448.
46. A. Harriman, V. Heitz, and J.-P. Sauvage (1993) *J. Phys. Chem.* **97**, 5940–5946.
47. G. J. Kavarnos (1993) *Fundamentals of Photoinduced Electron Transfer*, VCH, New York, pp. 287–342.
48. I. Rips and J. Jortner (1987) *J. Chem. Phys.* **87**, 2090–2099.
49. D. G. Johnson et al. (1993) *J. Am. Chem. Soc.* **115**, 5692–5700.
50. L. D. Zusman (1980) *Chem. Phys.* **49**, 295–302.
51. R. A. Marcus (1987) in J. Avery et al., (Eds.), *Understanding Molecular Properties*, D. Reidel, Dordrecht, The Netherlands, pp. 229–236.
52. V. N. Knyukshto et al. (1999) *Khim. Phys.* **18**, 30–39 (in Russian).
53. D. D. Fraser and J. R. Bolton (1994) *J. Phys. Chem.* **98**, 1626–1633.